Int. J. Solids Structures, 1974, Vol. 10, pp. 1069–1089. Pergamon Press. Printed in Gt. Britain.

PRISMATIC SHELLS WITH HEXAGONAL CROSS-SECTION†

DUSAN KRAJCINOVIC‡

(*Received* 13 *August* 1973; *revised* 27 *December* 1973)

Abstract—A new discrete-continuous analytical model for prismatic shells with hexagonal cross-section is developed on the basis of the semimembrane shell theory. Final results for stresses are derived in form of simple expressions. The proposed analytical model is checked against test and finite element results. The accuracy is judged to be exceptionally good in all cases examined. Therefore, it appears that the method provides a simple but powerful tool in design of nuclear reactor subassembly ducts.

NOTATION

A	cross-sectional area
$a_{ij}, b_{ij}, c_{kj}, r_{kh}, s_{kh}$	definite integrals (matrix elements) defined by (4.1.3)
E, G	elastic and shear modulus
F_i	functions in matrix (7.3)
h	shortest distance between shell middle surface and the centroidal axis
I	moment of inertia of a flat about its middle surface
$I_x, I_y, I_\omega, J_t, K$	moments of inertia of the hexagonal cross-section (4.1)
k	change of curvature
L	span
l	distance between two adjacent modes
M_z, M_s	bending moments
$m_{\omega n}, q_n$	nondimensional generalized forces (6.9)
N_z, N_s, N_{zs}	normal and shear forces
P	generalized force (6.1)
p_z, p_n, p_s	components of the external loading
p_{sj}, p_{zk}	load components associated with deformation modes Ψ_j or Φ_k
$p_{s(ij)}$	axial force in member (ij)
$\bar{p}_s, \bar{p}_z$	nondimensional load components (6.11)
Q	generalized shear force (6.4)
R	reactions of pinned supports
r, s, p_ω	nondimensional parameters (5.7)
$u(z, s), v(z, s)$	displacement components (Fig. 1)
$U_i(z), V_j(z)$	generalized coordinates
V_e	elastic strain energy
W	work of external loads
$[f]$	field (transfer) matrix (7.3)
$\{s_n\}$	state vector (7.2)
$\alpha, \beta, \gamma, \Delta, a_3, b_3$	parameters (7.4)
$\varepsilon_z, \varepsilon_s, \gamma_{zs}$	components of the strain tensor
$\Phi_i(s), \Psi_j(s)$	selected deformation modes (Figs. 2 and 3)
ν	Poisson's ratio
κ, ω	nondimensional generalized coordinates
$\sigma_z, \sigma_s, \tau_{zs}$	components of the stress tensor

† Work done under the auspices of the U.S. Atomic Energy Commission.

‡ Associate Professor, Department of Materials Engineering, University of Illinois at Chicago Circle; formerly Member of Technical Staff Argonne National Laboratory.

Superscripts

(b)	beam bending
(d)	distortion
(l)	local referring to the hex "frame" with pinned supports
(v)	distortion of the hex frame once the supports are removed.

1. INTRODUCTION AND BACKGROUND

According to the present design of a typical core for a Liquid Metal Fast Breeder Reactor, fuel pins are stored in subassembly ducts shaped as thin and slender prismatic shells with hexagonal cross-section. Elastic stresses in prismatic shells may be analyzed in a variety of ways depending on the desired level of accuracy and sophistication ranging from the beam theory[1] to complicated folded plate analyses[2, 3] and purely numerical techniques[4]. An inherent disadvantage of more accurate theories is that they are complex, time consuming and often require special skills. On the other side of the spectrum, beam theory underestimates longitudinal normal stresses and completely ignores hoop stresses. It was an out-of-reactor control-rod thimble failure[5] which clearly pointed out the inadequacy of the beam theory unable to offer a plausible explanation for the fracture. Therefore, it was proposed to develop a new method both simple and accurate enough to be used effectively by a practical designer.

According to the discrete–continuous model, developed in[6] for a truly special case of loading, the possible cause of the thimble failure[5] was excessive hoop stress. When the conclusions of this analysis were corroborated by actual metallurgical observation, it was decided to develop the analytical model to the extent enabling stress analyses for arbitrary systems of external loads. The practical importance of this effort lies in the fact that during both in and out-of-vessel handling, a can is actually subjected to a variety of loads. Moreover, many problems auxiliary to the solution of the entire core restraint problem demand an adequate analytical study. The results of such studies will be incorporated in the final computer code.

A rather extensive series of tests† and numerical computations was performed in order to verify the analytical results. Some of the test results are listed in the sequel and compared with analytically obtained data. The accuracy is judged to be good and the conclusion is that the analytical model presents a reliable design tool.

2. ELASTIC STRESS ANALYSIS

Analytical model

Solution of a prismatic shell problem, according to the conventional theory, is contingent on the ability to resolve the governing system of partial differential equations. Since the governing system of equations, in general case, does not allow an analytical solution, a host of various simplified computational models[2] were introduced in connection with specific problems.

An essential feature of the deformation of a long, slender prismatic shell is that the variation of all kinematic variables is much more pronounced along the circumference than in the direction of generators. Therefore, change of curvature of generators (also moments M_z and transverse forces Q_z) and the twisting of the middle surface (and torques M_{sz}) are negligible, in comparison with other kinematic magnitudes, except in the proximity of

† Tests were performed by Dr. J. E. Flinn of the EBR-II Division, Argonne West, Idaho, U.S.A.

discontinuities (such as concentrated forces or supports). Consequently, it appears reasonable to model the actual shell (Fig. 1a) by a discrete–continuous system (Fig. 1 bottom)[6, 7] consisting of an infinite number of hexagonal frames interconnected by a lattice transmitting the nonvanishing membrane forces N_z and N_{zs}. It was demonstrated[8] that such a semi-membrane analytical model† may be obtained from the exact shell theory by neglecting second order derivatives with respect to z in comparison with second order derivatives with respect to s.

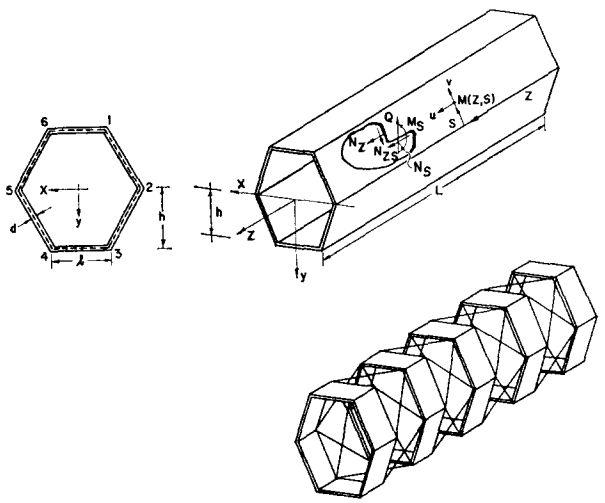

Fig. 1. Prismatic shell with a hexagonal cross-section and the analytical discrete continuous model.

3. GOVERNING EQUATIONS

The total elastic strain energy V_e of the selected discrete–continuous system shown in Fig. 1(b) consists of two parts: strain energy of the hexagonal "frame" in flexure and the strain energy of the connecting "lattice". Thus,

$$V_e = \frac{1}{2}\int_0^L \int_s (N_s \varepsilon_s + M_s k_s + N_z \varepsilon_z + N_{zs}\gamma_{zs})\, \mathrm{d}s\, \mathrm{d}z \tag{3.1}$$

where N_z, N_s and N_{zs} are normal and shear forces, M_s the bending moment (Fig. 1), while ε_s, ε_z and γ_{zs} are normal and shear strains and k_s the change in curvature. Integration domain in (3.1) is over the entire middle surface of the shell (with L being the shell length measured along the generator).

It is further convenient to decompose the in-plane deformation of the frame into two parts: local bending under the action of external load for which the nodal displacements vanish, and the global distortion associated with the differential (relative) displacements of 6 nodes. Therefore, we first fix each node by means of a pinned support to compute the local strain energy (i.e. change of curvature $k_s^{(l)}$) of the frame and support reactions $R^{(l)}$ due to external loading. Next, we remove the supports and apply the negative reactions $-R^{(l)}$ as actions to compute the component of the strain energy (i.e. $k_s^{(v)} = k_s - k_s^{(l)}$) associated

† In addition, range of the applicability of the model is discussed in the same Reference.

with the differential displacement sof nodes.† Note also that the local bending ($k_s^{(v)} = 0$) characterized by zero nodal displacement does not involve stressing of the connecting lattice (i.e. $N_z \equiv N_{zs} \equiv 0$). From (1) we can now write

$$V_e = \frac{1}{2}\int_0^L \int_s (N_s \varepsilon_s + M_s^{(l)} k_s^{(l)} + N_z \varepsilon_z + N_{zs}\gamma_{zs} + M_s^{(v)} k_s^{(v)})\, ds\, dz \tag{3.2}$$

where $M_s^{(l)}$ are the bending moments in the hex frame with pinned nodes, while $M_s^{(l)} = M_s - M_s^{(l)}$ are the moments associated with the differential displacements of nodes (global distortion of the hexagon).

Quite naturally, the treatment of external loads should be consistent with the model. The load components p_s and p_z are transmitted directly to lattice members. The work of the load component p_n normal to the middle surface consists of two parts. The first component of the work is associated with the local bending (reflected through displacements $w^{(l)}$) of the pinned "frame." Additional work is done by reactions $-R^{(l)}$ (decomposed‡ into components $p_{s(ij)}$ in direction of "frame" members) on the distortion of the frame (defined by displacements $v_{(ij)}$ in direction of individual members connecting nodes i and j) once the supports are removed.

$$W = \int_0^L \int_s (p_z u + p_s v + p_n w)\, ds\, dz = \int_0^L \int_s (p_z u + p_s v + p_n w^{(l)})\, ds\, dz + \int_0^L \sum_{ij=1}^{6} p_{s(ij)} v_{(ij)}. \tag{3.3}$$

In the case of concentrated loads all integrals are to be taken in the Stieltjes sense.

Next, we have to establish the relation between the displacement of an arbitrary point on the middle surface and the displacement components of six nodes. For convenience, with the exception of local bending (of the "frame" with supported nodes) we postulate that for each cross-section $z = z_k$ componental displacements $u(z_k, s)$ and $v(z_k, s)$ are piece-wise smooth, linear functions of s, i.e. polygonal graphs with vertices in nodal points. Thus, the displacement components of an arbitrary point of middle surface can be written as finite sums

$$u(z, s) = \sum_{i=1}^{n_u} U_i(z)\Phi_i(s) \tag{3.4}$$

$$v(z, s) = \sum_{j=1}^{n_v} V_j(z)\Psi_j(s)$$

where $U_i(z)$ and $V_j(z)$ are unknown generalized coordinates and $\Phi_i(s)$, $\Psi_j(s)$ *a priori* selected (in accord with the postulate of the linearity of u and v between two nodes) deformation modes. Mathematically, this leads to the reduction of the system of partial differential equations to a system of ordinary differential equations[11].

In the general case the number of degrees-of-freedom of a hexagonal kinematic chain§ is obviously 12 ($n_u = n_v = 6$). Every node (i) can be given a unit out-of-plane displacement $u_i = 1$ ($u_j = 0, j \neq 1$) and/or every plate (k, $k + 1$) can be given a unit in-plane displacement $v_k = 1$ for which all the nodes except k and $k + 1$ are fixed.

† We note here that this represents a significant difference of the present model from the model introduced by Vlasov [7, 9]. The present model has an apparent physical explanation and enables the consideration of the general case of loading.

‡ This course of action parallels in a certain sense the so-called Gruber's method [10]. The subsequent procedure is, however, entirely different.

§ For convenience, we consider the members to be inextensional. In other words, we assume $\varepsilon_s \sim 0$.

From (3.4) it follows that the strains are

$$\varepsilon_z = u_{,z} = \sum_{i=1}^{6} U_{i,z}\Phi_i$$

$$\varepsilon_s = v_{,s} = \sum_{j=1}^{6} V_j \Psi_{j,s} \sim 0 \tag{3.5}$$

$$\gamma_{zs} = u_{,s} + v_{,z} = \sum_{i=1}^{6} U_i \Phi_{i,s} + \sum_{j=1}^{6} V_{j,z}\Psi_j .$$

Accordingly, the stress resultants are

$$N_z = \frac{Ed}{1-\nu^2}(\varepsilon_z + \nu\varepsilon_s) = \frac{Ed}{1-\nu^2}\left(\sum_i U_{i,z}\Phi_i + \nu\sum_j V_j\Psi_{j,s}\right)$$

$$N_s = \frac{Ed}{1-\nu^2}(\varepsilon_s + \nu\varepsilon_z) = \cdots N_{zs} = Gd\gamma_{zs} = \cdots \tag{3.6}$$

where comma in the index indicates the differentiation with respect to the variable following; E and G are elastic and shear moduli, d the thickness of each strip and ν the Poisson's ratio.

Finally, we consider the bending moments M_s due to the deformation of the hex "frame" in its plane. With each deformation mode $\Psi_j = 1$ associated is a moment field M_{sj} in the "frame." Consequently, for the deformation $V_j\Psi_j$ the moments are, according to the linear theory, $M_{sj}V_j$. Thus, the "frame" strain energy reads

$$\frac{1}{2}\int M_s^{(v)} k_s^{(v)}\,\mathrm{d}s = \frac{1}{2}\int \frac{1}{EI}\left(\sum_{j=1}^{6} V_j M_{sj}^{(v)}\right)\mathrm{d}s \tag{3.7}$$

where $I = bd^3/12$ is the moment of inertia of a frame member of unit width $b = 1$.

Substitution of (3.5–3.7) into (3.2) leads in conjunction with (3.3) to

$$\begin{aligned} V_e - W = \int_0^L \int_s \Bigg\{ & \frac{Ed}{2(1-\nu^2)}\left[\sum_i (U_{i,z}\Phi_i)^2 + \sum_j (V_j\Psi_{j,s})^2\right] \\ & + 2\nu\sum_i U_{i,z}\Phi_i \sum_j V_j\Psi_{j,s} + \frac{Ed}{4(1+\nu)}\left(\sum_i U_i\Phi_{i,s} + \sum_j V_{j,z}\Psi_j\right)^2 \\ & + \frac{1}{EI}\left(\sum_j V_j M_{sj}^{(v)}\right)^2 - p_z\sum_i U_i\Phi_i - p_s\sum_j V_j\Psi_j\Bigg\}\,\mathrm{d}s\,\mathrm{d}z \\ & - \int_0^L V_j \sum_{ij} p_{s(ij)}\Psi_{h(ij)}\,\mathrm{d}z + \int_0^L\int_s (M_s^{(l)}k_s^{(l)} + p_n w_n^{(l)})\,\mathrm{d}s\,\mathrm{d}z \end{aligned} \tag{3.8}$$

or, in short

$$V_e - W = f_1(z, U_i, U_{i,z}, V_j, V_{j,z}, p_s, p_z) + f_2(z, p_n) \tag{3.9}$$

where f_2 is the strain energy associated with the local flexure of the "frame" with pinned supports. Obviously f_2 is not the function of nodal displacements U_i, V_j and their derivatives and can be treated separately.

The Euler equations minimizing the integrals (3.8) can be written in the form of a quadratic matrix ($j + h = i + k = 6 + 6 = 12$)

$$\begin{bmatrix} a_{ij}D^2 - \frac{1-\nu}{2} b_{ij} & -\frac{1-\nu}{2} c_{kj} D \\ -\frac{1-\nu}{2} c_{ih} D & \frac{1-\nu}{2} r_{kh} D^2 - s_{kh} \end{bmatrix} \begin{bmatrix} U_i \\ V_k \end{bmatrix} = \frac{1-\nu^2}{E} \begin{bmatrix} p_{zj} \\ p_{sh} \end{bmatrix} \tag{3.10}$$

$$(i, j, k, h = 1, 2, \ldots, 6)$$

where $D^n = \frac{\mathrm{d}^n(\ )}{\mathrm{d}z^n}$ is a differential operator. The constant terms multiplying unknown generalized coordinates U_i, V_k in (3.10) are definite integrals defined as follows

$$a_{ij} = \int_A \Phi_i \Phi_j \, \mathrm{d}A \qquad b_{ij} = \int_A \Phi_{i,s} \Phi_{j,s} \, \mathrm{d}A$$

$$c_{jk} = \int_A \Phi_{j,s} \Psi_k \, \mathrm{d}A \qquad r_{hk} = \int_A \Psi_h \Psi_k \, \mathrm{d}A \tag{3.11}$$

and

$$s_{hk} = \frac{1+\nu^2}{E} \int \frac{M_k M_h}{EI} \, \mathrm{d}s.$$

The load terms are

$$p_{zj} = \int_s p_z \Phi_j \, \mathrm{d}s \qquad p_{sh} = \int_s p_s \Psi_h \, \mathrm{d}s + \sum_{(ij)=1}^{6} p_{s(ij)} \Psi_{h(ij)}. \tag{3.12}$$

The integration domain is either the entire cross-sectional area $\mathrm{d}A = (\mathrm{d}s)d$ or the circumference s.

The boundary conditions are

$$\int_s N_z \Phi_j \, \mathrm{d}s = 0 \qquad \int_s N_{zs} \Psi_h \, \mathrm{d}s = 0. \tag{3.13}$$

Equations (3.10) do not include local bending of the "frame" with pinned supports which will be handled separately using routine methods of frame analysis.

4. SELECTION OF DEFORMATION MODES

The basic feature of the method developed is that the structure is approximated by a continuous–discrete model stipulating the kinematics of the cross-sectional deformation. An arbitrary displacement field $u(z, s)$ and/or $v(z, s)$ is approximated by a polygonal graph (linear periodic spline function) with vertices in nodal points. The necessary condition enabling the description of a general case of such a spline function is that the modes $\Phi_i(s)$ and $\Psi_j(s)$ are selected as independent functions (say, forming a complete set of cardinal splines). Obviously, the choice is not unique. In order to simplify the governing equations (3.10) it makes sense to select both sets of functions $\Phi_i(s)$ and $\Psi_j(s)$ as orthogonal rendering submatrices (3.11) as sparse as possible.

For a better physical understanding we select first 6 generalized coordinates U_i and V_k ($i, k = 1, 2, 3$) as 3 displacements and 3 rotations of a rigid (distortionless) cross-section.

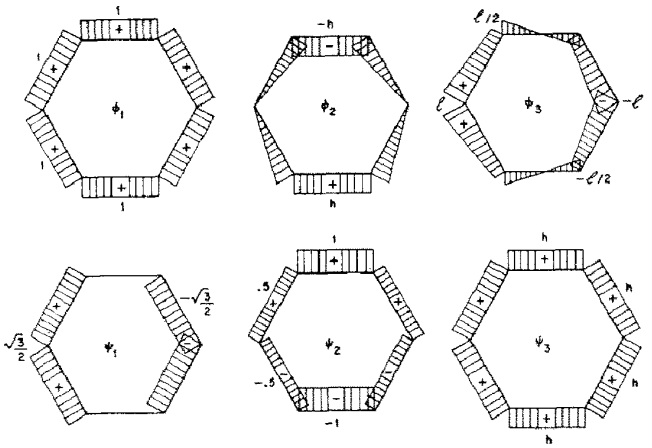

Fig. 2. Six lowest (beam) deformation modes.

Corresponding modes Φ_i and Ψ_j are diagrammed in Fig. 2. The remaining 6 generalized coordinates, reflecting the distortion of the cross section and, consequently, deviation from the beam theory are selected so that the modes Φ_i and Ψ_k $(i, k = 4, 5, 6)$ (Fig. 3) are orthogonal with respect to the modes shown in Fig. 2.

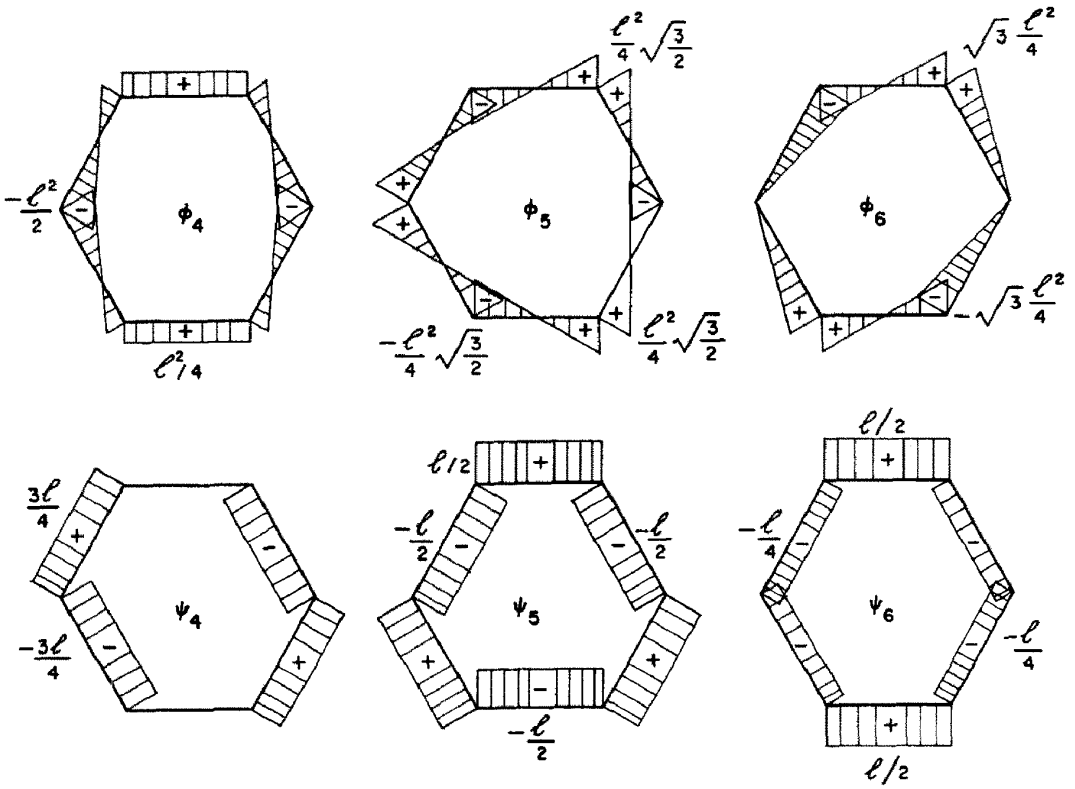

Fig. 3. Six deformation modes characterized by the cross-sectional distortion.

Having established a set of orthogonal functions $\Phi_i(s)$ and $\Psi_k(s)$ we compute definite integrals (3.11). It is quite remarkable that even matrices b_{ij} and c_{jk} turn out diagonal minimizing the number of terms in (3.10). The non-zero elements are

$$\begin{aligned}
&a_{11} = 6dl = A \qquad\qquad a_{22} = a_{33} = \tfrac{5}{2}dl^3 = I_x = I_y \\
&a_{44} = 2a_{55} = a_{66} = \tfrac{3}{8}dl^5 = I_\omega \\
&r_{11} = r_{22} = b_{22} = b_{33} = c_{22} = c_{33} = 3dl = \tfrac{1}{2}A \\
&r_{44} = r_{55} = r_{66} = b_{44} = b_{55} = b_{66} = -c_{44} = -c_{55} = -c_{66} = \tfrac{9}{4}dl^3 = K \\
&r_{33} = 3\sqrt{3}\,dl^2 = J_t .
\end{aligned} \tag{4.1}$$

The meaning of these coefficients is in view of the selections of generalized coordinates quite obvious. Multiplied by E (or G) a_{11} is, for example, rigidity with respect to axial deformation; a_{22} and a_{33} to pure bending; r_{33} to torsion; r_{11}, r_{22}, b_{22} and b_{33} to shear; a_{44}, a_{55}, a_{66} to out-of-plane distortions; and r_{44}, r_{55} and r_{66} to in-plane distortions.

Finally, using routine methods of structural analysis (i.e. Castigliano's principle) we compute each integral s_{hk} (3.11) as a generalized elastic reaction of the hth constraint of the "frame," associated with the in-plane deformation (distortion) defined by $V_k = 1$ and $V_n = 0$ $(n \neq k)$. Since first three modes Ψ_i $(i = 1, 2, 3)$ are associated with distortionless rigid plane motion $s_{hk} = 0$ whenever one of its indices is less than or equal to 3.

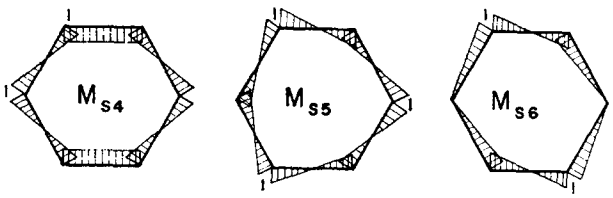

Fig. 4. Frame bending moments corresponding to distortions $\Psi_j (j = 4, 5, 6)$. Moments multiplied by $8/p_n l^2$.

Diagram of bending moments corresponding to distortionless $V_k = 1$, $V_j = 0$ $(j \neq k)$ is plotted in Fig. 4. For $k = 4$ the bending moments in the nodes are

$$M_{j4} = \frac{\delta_{4\psi}}{\int \frac{M_4^2}{EI}\,ds} = \frac{8\,\frac{2h}{l}}{\frac{10}{3}\,\frac{l}{EI}} = \frac{24}{5}\,\frac{hEI}{l^2}. \tag{4.2}$$

In an identical way

$$M_{55} = M_{66} = \frac{2\sqrt{3}\,EI}{l}.$$

From (3.11) it follows

$$s_{44} = \frac{24}{5}\,\frac{d^3}{l} = J = \frac{5}{12}\,s_{55} = \frac{5}{12}\,s_{66}. \tag{4.3}$$

Again, all elements off the main diagonal vanish, i.e. the submatix s_{hk} is also diagonal.

5. GOVERNING EQUATIONS

Due to the fact that all matrices (3.11) are diagonal, governing equations (3.10) are uncoupled into several blocks and it is possible to write them explicitly.

5.1 *Axial loading*

The equation $j = 1$ in (3.10) is completely uncoupled and with $U_1 = u_0$ reads

$$EAu_{0,zz} = (1 - \nu^2)p_1 \tag{5.1}$$

which is the well known column equation.

5.2 *Bending in* yz *plane*

Equations $j = 2$ and $h = 1$ in (3.10) are coupled. Using new symbol $V_1 = \eta_y$ and eliminating U_2 follows the well known equation of beam in flexure

$$EI_y \eta_{y,zzzz} = p_{s1} - 2\frac{EI_y}{GA} p_{s1,zz} + p_{z2,zz}. \tag{5.2}$$

5.3 *Bending in* xz *plane*

Equations $j = 3$ and $h = 2$ in (3.10) are also coupled. Using $V_2 = \eta_x$ and eliminating U_3 follows again the equation for a beam in flexure

$$EI_x \eta_{x,zzzz} = p_{s2} - 2\frac{EI_x}{GA} p_{s1,zz} + p_{z3,z}. \tag{5.3}$$

5.4 *Torsion*

Equation $h = 3$ in (3.10) is uncoupled and after substitution $V_3 = \theta_2$ follows the well known torsion equation

$$GJ_t \theta_{z,zz} = -p_{s3}. \tag{5.4}$$

We note that the torsion is not associated with normal stresses σ_z. This is the consequence of the fact that the sectorial coordinate vanishes, i.e. that the product hd (thickness multiplied by the distance to the shear center) is equal for all plates ([12], Chap. V.2).

5.5 *Shell-like deformation*

The remaining six deformation modes reflecting the deviation from the beam theory (characterized by the cross-sectional distortion) are grouped into three pairs ($j = h = 4, 5, 6$). For example, for $j = h = 4$ from (3.10) it follows

$$\begin{aligned} &EI_\omega U_{4,zz} - (1 - \nu)GK(U_4 - V_{4,z}) + (1 - \nu^2)p_{z4} = 0 \\ &-(1 - \nu)GK(U_{4,z} - V_{4,zz}) - EJV_4 + (1 - \nu^2)p_{s4} = 0. \end{aligned} \tag{5.5}$$

Introducing the non-dimensional variable $\omega_y = lU_4$ after elimination of V_4 it follows

$$\omega_m^{1v} - 2r_m^2 \omega_m'' + s_m^4 \omega_m = p_{\omega m} \qquad (m = y) \tag{5.6}$$

where the differentiation is with respect to $\xi = z/L$. Nondimensional parameters r_y, s_y and the loading term $p_{\omega y}$ are

$$r_y^2 = \frac{(1+\nu)J}{(1-\nu)K}L^2 = \frac{32(1+\nu)}{15(1-\nu)}\left(\frac{d}{l}\right)^2\left(\frac{L}{l}\right)^2$$

$$s_y^4 = \frac{J}{I_\omega}L^4 = \frac{64}{5}\left(\frac{d}{l}\right)^2\left(\frac{L}{l}\right)^4 \tag{5.7}$$

$$p_{\omega y} = \frac{1-\nu^2}{EI_\omega}L^2 l(p'_{s4} - p''_{z4}) + \frac{(1+\nu)J}{GKI_\omega}lL^4 p_{z4}.$$

For $j = h = 5$ and 6 only terms by U_m'' in (5.5a) and by U_m in (5.5b) differ by a constant. Introducing notation $\omega_x = U_5 l$ and $\omega_z = U_6 l$, and eliminating V_5 and V_6 obtained is again equation (5.6) with $m = x, z$ consecutively. Parameters are

$$r_m^2 = \tfrac{5}{4}r_y^2 \qquad s_m^2 = \tfrac{5}{4}s_y^2$$

$$p_{\omega m} = \frac{1-\nu^2}{EI_\omega}L^2 l(Lp'_{sj} - p''_{zj}) + \frac{5}{4}\frac{(1+\nu)J}{GKI_\omega}lL^4 p_{zj} \tag{5.8}$$

where for $m = x, j = 5$ and for $m = 2, j = 6$.

In conclusion, as a result of our choice of deformation modes:

(a) the method is formulated as an extension of the conventional beam theory,

(b) the governing system of 12 simultaneous differential equations (3.10) is decoupled into five separate pairs and two independent equations all with a definite physical meaning.

The solution of governing equations derived is either routine (4.1–4) or simple (5.6). In the sequel we concentrate exclusively on the solution of the equation (5.6) governing the shell-like behavior of our folded structure.

6. GENERALIZED FORCES AND STRESSES

Analogous to the conventional beam theory let us introduce the generalized force in the form

$$P_j(z) = \int_A \sigma_z(z, s)\Phi_j(s)\,\mathrm{d}A \tag{6.1}$$

which for $\nu = 0$, using (3.4, 5, 11) can be rewritten as

$$P_j(z) = E\sum_{i=1}^{6} U_{i,z}\int_A \Phi_i\Phi_j\,\mathrm{d}A = Ea_{jj}U_{j,z}. \tag{6.2}$$

Solving for $U_{j,z}$, substituting into (3.5) and using the Hooke's law $\sigma_z = E\varepsilon_z$ it follows that

$$\sigma_z(z, s) = \sum_{i=1}^{6}\frac{P_i(z)}{a_{ii}}\Phi_i(s) = \frac{N_z}{A} + \frac{M_x}{I_x}x + \frac{M_y}{I_y}y + \sum_{i=4}^{6}\frac{P_i}{a_{ii}}\Phi_i. \tag{6.3}$$

First three terms constitute the familiar Strength of Materials formula, while the sum (last three terms) reflects the contribution associated with the cross-sectional distortion.

We also introduce the generalized shear force

$$Q_j(z) = \int_A \tau_{zs}(z, s)\Psi_j(s)\,\mathrm{d}A = G(c_{ij}U_i + r_{hj}V_{h,z}), \tag{6.4}$$

such that

$$\tau_{zs} = \tau_{zs}^{(\text{beam})} - GK \sum_{h=4}^{6} (U_h - V_{h,z}). \tag{6.5}$$

From (6.1, 3) and (5.5a) (and two similar ones for $j = 5, 6$) it follows for $v = 0$ that

$$P_{j,z} = -Q_j \qquad (j = 4, 5, 6). \tag{6.6}$$

Therefore, generalized forces P_j and Q_j are related exactly in the same way as bending moments and transverse forces (i.e. P_j and Q_j for $j = 2, 3$) in the conventional beam theory.

We also define function V_j and generalized forces P_j and Q_j ($j = 4, 5, 6$) in terms of ω_j. From (6.1, 6) it follows

$$Q_j = -Ea_{jj} U_{j,zz} \tag{6.7}$$

while from (5.5a, b) it can be derived

$$V_n = -s_n^4 \omega_n''' \qquad (n = x, y, z) \tag{6.8}$$

where the index 4 turns into y, 5 into x and 6 into z. Introducing non-dimensional quantities

$$\kappa_n = \frac{l}{L} s_n^4 V_n \qquad m_{\omega n} = \frac{P_n}{Ea_{nn}} Ll \qquad q_n = \frac{Q_n}{Ea_{nn}} L^2 l \tag{6.9}$$

it follows

$$m_{\omega n} = \omega_n' \qquad q_n = -\omega_n'' - \bar{p}_{zn} \qquad \kappa_n = -\omega_n''' + \bar{p}_{sn} + \bar{p}_{zn} \tag{6.10}$$

where again $n = x$ or 5, y or 4, z or 6. The non-dimensional load terms read

$$\bar{p}_{zn} = p_{zn} \frac{lL^2}{Ea_{nn}} \bar{p}_{sn} = p_{sn} \frac{lL^3}{Ea_{nn}}. \tag{6.11}$$

The normal stresses in the frame are

$$\sigma_s = \frac{p_{si}}{d} + \frac{M_s^{(v)}}{I} \zeta + \sum_{j=4}^{6} V_j \frac{M_{sj}^{(l)}}{I} \zeta \tag{6.12}$$

where ζ is the local coordinate measured from the middle plane of each plate in the direction of its normal. First two terms reflect the contribution of the local bending of the "frame" with pinned nodes, while the sum represents circumferential normal stresses due to the gross cross-sectional distortion (i.e. relative displacement of "frame" nodes).

7. SOLUTION OF THE GOVERNING EQUATION

The solution of (5.6) in terms of four arbitrary constants and a combination of trigonometric and hyperbolic functions is routine. For our purposes it is advantageous to employ the method of initial parameters [6, 13], i.e. to present the solution in terms of four constants ω_n^0, κ_n^0, $m_{\omega n}^0$, $q_n^0 (n = x, y, z)$ being the values of four functions (6.10) at $z = 0$. After some elementary derivation[6] obtained is the matrix relation

$$\{s_n\}_\xi = [F(\xi)]\{s_n^0\} + \{s_n^p\} \qquad (n = x, y, z) \tag{7.1}$$

where $\{s_n\}_\xi$ is the state vector

$$\{s_n\}_\xi = [\omega_n, \kappa_n, m_{\omega n}, q_n]^t \tag{7.2}$$

taken at cross-section ξ (superscript t standing for transposition). The field transfer matrix $[F(\xi)]$ reads

$$[F] = \begin{bmatrix} F_2 - \gamma F_4 & -\Delta(\alpha F_1 - \beta F_3) & \Delta(b_3 F_3 - a_3 F_1) & -\dfrac{1}{2\alpha\beta} F_4 \\ \dfrac{(\alpha^2+\beta^2)^2}{2\alpha\beta} \times (\alpha F_1 + \beta F_3) & F_2 + \gamma F_4 & \dfrac{(\alpha^2+\beta^2)^2}{2\alpha\beta} F_4 & \dfrac{1}{2\alpha\beta}(a_3 F_1 + b_3 F_3) \\ -\dfrac{\alpha^2+\beta^2}{2\alpha\beta} \times (\beta F_1 - \alpha F_3) & -\dfrac{1}{2\alpha\beta} F_4 & F_2 - \gamma F_4 & \dfrac{-1}{2\alpha\beta}(\alpha F_1 + \beta F_3) \\ \dfrac{(\alpha^2+\beta^2)^2}{2\alpha\beta} F_4 & \dfrac{1}{2\alpha\beta}(\alpha F_1 + \beta F_3) & \dfrac{\alpha^2+\beta^2}{2\alpha\beta}(\alpha F_1 - \beta F_3) & F_2 + \gamma F_4 \end{bmatrix}. \tag{7.3}$$

Functions $F_i(\xi)$ in (7.3) are defined as follows

$$F_1(\xi) = \cosh \alpha\xi \sin \beta\xi \qquad F_3(\xi) = \sinh \alpha\xi \cos \beta\xi$$
$$F_2(\xi) = \cosh \alpha\xi \cos \beta\xi \qquad F_4(\xi) = \sinh \alpha\xi \sin \beta\xi$$

with

$$\alpha = \frac{1}{4}(s^2 + r^2)^{1/2} \qquad \beta = \frac{1}{4}(s^2 - r^2)^{1/2}$$
$$a_3 = \alpha(\alpha^2 - 3\beta^2) \qquad b_3 = \beta(3\alpha^2 - \beta^2) \tag{7.4}$$
$$\gamma = \frac{\alpha^2 - \beta^2}{2\alpha\beta} \qquad 1/\Delta = 2\alpha\beta(\alpha^2 + \beta^2).$$

Further, $\{s_n^0\}$ is the state vector (7.2) taken at $\xi = 0$ and $\{s_n^p\}$ the vector of particular solutions [6] given by

$$\{s_n^p\}_\xi = \int_0^\xi [F_n(\xi - \eta)]\{s_n^*(\eta)\}\, d\eta \tag{7.5}$$

where $\{s^*\}$ is the vector of external loads $(m_{\omega n}^*, \kappa_n^*)$ and externally induced distortions (ω_n^*, κ_n^*) of known magnitude. The integral in (7.5) is again understood in Stieltjes' sense in case of concentrated loads.

8. SPECIAL CASES

After all the necessary relations are derived we can discuss the application of the method on a few particular cases.

Firstly, we illustrate the determination of the load terms representing the right hand side of (3.10) for several common cases of loading. Consider a uniformly distributed load p_n in the direction of the normal to the upper flat (Fig. 5a). We begin with the local bending of the "frame" with pinned supports. Using routine methods of frame analysis computed are the bending moments $M_s^{(i)}$ (Fig. 5a) and the support reactions (Fig. 5b)

$$R_1' = \frac{p_n l}{2} \qquad R_1'' = R_2' = \frac{p_n l}{15} \qquad R_2'' = R_3 = \frac{p_n l}{60}.$$

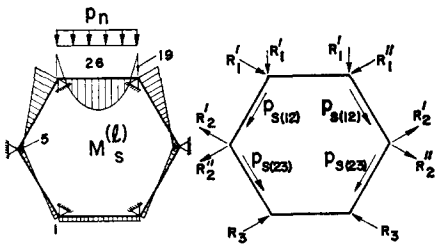

Fig. 5. Decomposition of external load p_n. All moments multiplied by $360/p_n l^2$.

These reactions (Fig. 5b) are subsequently decomposed into components $p_{s(ij)}$ in direction of the "frame" members

$$p_{s(12)} = \frac{\sqrt{3}}{3}(R_1'' + 2R_1' + R_2' + 2R_2'') = \frac{7\sqrt{3}}{18} p_n l$$

$$p_{s(23)} = -\frac{\sqrt{3}}{3}(2R_2' + R_2'' + R_3) = -\frac{\sqrt{3}}{18} p_n l$$

where the subscript (ij) refers to the nodes i and j connected by the flat in question. Next, the only two non-vanishing load terms are calculated from (3.12)

$$p_{s1} = \frac{2\sqrt{3}}{3}\left(\frac{7\sqrt{3}}{18} - \frac{\sqrt{3}}{18}\right) p_n l = p_n l$$

$$p_{s4} = 2\frac{3l}{4}\left(\frac{7\sqrt{3}}{18} + \frac{\sqrt{3}}{18}\right) p_n l = \frac{2\sqrt{3}}{3} p_n l^2. \tag{8.1}$$

The load p_{s1}, as expected, represents the resulting transverse force associated with the bending in (yz) plane. The self-equilibrated load component p_{s4}^* is the cause of the cross-sectional distortion typified by deformation modes Φ_4 and Ψ_4.

Analogously, forces p_{sj} are computed for a variety of load cases (Table 1).

Table 1. Determination of load terms p_{sj} for various external nodal loads Q_{tm}

External load	Load terms p_{sj}						Governing equation
	p_{s1}	p_{s2}	p_{s3}	p_{s4}	p_{s5}	p_{s6}	
$Q_{1y}^* = Q_{6y}^* = 1$	2			$2h$			(5.2; 5.6y)
$Q_{1y}^* = -Q_{6y}^* = 1$			l		$-2h$	$-4h/3$	(5.4; 5.6xz)
$Q_{5x}^* = 1$		1		$3l/2$	$-l$		(5.3; 5.6yx)
$Q_{4x}^* = Q_{6x}^* = 1$		2			l		(5.3; 5.6x)
$Q_{4x}^* = -Q_{6x}^* = 1$			$-2h$			l	(5.4; 5.6z)
$Q_{2x}^* = -Q_{5x}^* = 1$				$3l$			(5.6y)

† Note that term p_{sj} is, in fact, virtual work associated with virtual displacement $\Psi_j = 1$, $\Psi_i = 0$ $(i \neq j)$.

In Table 1, $Q_{jx}^* = -R_{jx}^*$ is an external point or line force in direction of positive x-axis acting on the node j. First three load terms $p_{si} (i \leq 3)$ are two transverse forces and the torque. Node numbers are as shown in Fig. 1.

In order to compute p_{sj} for an external force with a component in direction of the shell axis z we simply use (3.12a). For example, consider a concentrated point or line force $p_z^* = P^*(s - s_0)$ applied at the node 1. Then, from (3.12a) and Figs. 2 and 3, $p_{z1} = P^*$, $p_{z2} = -hP^*$, $p_{z3} = -\frac{l}{2} P^*$, $p_{z4} = \frac{l^2}{4} P^*$, $p_{z5} = \frac{l^2}{4} P^* \sqrt{\frac{3}{2}}$ and $p_{z6} = \frac{l^2}{4} P^* \sqrt{3}$. We immediately recognize first three terms to be the external normal force and two bending moments associated with the beam theory.

Once the load terms are established we turn our attention to determination of boundary conditions. First we have boundary conditions on u_0, η_y, η_x and θ_z and their derivatives characteristic of the conventional beam theory. Together with (5.1, 4) they form boundary value problems well known from the elementary structural mechanics.

In addition we have boundary conditions associated with (5.6), reflecting the nature of cross-sectional constraint (or the lack of it) at the shell ends. From (3.13b) and (6.5) it turns out that either a distortion or a corresponding generalized force must vanish at the terminal cross-section. There are essentially three ways in which the cross-section may be constrained:

(a) It may be completely free to distort, when, $m_{\omega n} = q_n = 0$; (8.2)

(b) It may be braced so that the relative in-plane displacements of all nodes vanish (thin diaphragm), when, $m_{\omega n} = \kappa_n = 0$; (8.3)

(c) It may be braced so that it remains a rigid plane (heavy diaphragm), when, $\omega_n = \kappa_n = 0$. (8.4)

As before, the index $n = x, y, z$.

It may frequently be computationally convenient to use symmetry about the midspan $z = L/2$. For distributed loads it follows that the odd functions vanish, i.e.

$$\omega_n = q_n = 0. \tag{8.5}$$

Finally we analyze the case of an external force $p_{sj}^* = P_{sj}^* \delta(z - L/2)$ concentrated at the midspan (δ stands for the Dirac-delta function while $j = 4, 5, 6$). With $1 - \nu^2 \approx 1$ from (5.5a) and (6.4) it follows

$$Q_{j,z} - EJV_j + P_{sj}^* \delta(z - L/2) = 0. \tag{8.6}$$

The term P_{sj}^* is, of course, determined from the Table 1. Integration of (8.6) over a small interval $\frac{L^-}{2}, \frac{L^+}{2}$ leads to

$$-Q_j] + P_{sj}^* = 0 \qquad (j = 4, 5, 6) \tag{8.7}$$

where the bracket denotes the jump in magnitude of Q_j at $z = L/2$. According to (8.7) the distortional load P_{sj}^* and the generalized force Q_j are related exactly as the transverse load and the concentrated transverse force in the conventional beam theory. Making use of non-dimensional quantities (6.1, 11) it folows

$$-q_j^+ = q_j^- = \tfrac{1}{2}\bar{P}_{sj}^*. \tag{8.8}$$

Condition (8.8), obviously, should be used in addition to (8.5a) in case of symmetry about $z = L/2$.

We can now proceed and examine the case of a shell free to distort at both ends (8.2) and loaded with a concentrated distortional load P^*_{s4} at the midspan.† The boundary conditions are (8.2, 5, 8)

$$m_{\omega y} = q_y = 0 \qquad \text{at} \quad \xi = 0$$
$$\omega_y = 0 \qquad q_y = \tfrac{1}{2}\bar{p}^*_{s4} \qquad \text{at} \quad \xi = 1$$

where $\xi = 2z/L$. We now use the matrix equation (7.1) to compute the two nonvanishing initial parameters ω_{y0} and κ_{y0}. From (7.3) it follows

$$\begin{bmatrix} F_2 - \gamma F_4 & \dfrac{\alpha F_1 - \beta F_3}{-2\alpha\beta(\alpha^2+\beta^2)} \\ \dfrac{(\alpha^2+\beta^2)^2 F_4}{2\alpha\beta} & \dfrac{\alpha F_1 + \beta F_3}{2\alpha\beta} \end{bmatrix} \begin{bmatrix} \omega_{y0} \\ \\ \kappa_{y0} \end{bmatrix} = \frac{1}{2}\bar{p}^*_{s4} \begin{bmatrix} 0 \\ \\ 1 \end{bmatrix} \tag{8.9}$$

where all functions F_i are evaluated for $\xi = 1$.

We further note that for slender, thinwalled shells the ratio $(s/r)^2 = 1.677(l/d) \gg 1$ is always large compared with unity. Therefore, from (8.9) it follows

$$\omega_{y0} \simeq \frac{\sin\beta - \cos\beta}{2\alpha^2} e^{-\alpha}\bar{p}^*_{s4} \qquad \kappa_{y0} = (2\alpha\cos\beta)e^{-\alpha}\bar{p}^*_{s4}.$$

Thus, at an arbitrary cross-section

$$\kappa_y(\xi) = \alpha e^{-\alpha}\{(\sin\beta - \cos\alpha)[F_1(\xi) + F_3(\xi)] + 2F_2(\xi)\cos\beta\}\bar{p}^*_{s4}$$
$$m_{\omega y}(\xi) = -\frac{e^{-\alpha}}{2\alpha}\{(\sin\beta - \cos\beta)[F_1(\xi) - F_3(\xi)] + 2F_4(\xi)\cos\beta\}\bar{p}^*_{s4}. \tag{8.10}$$

As shown in Fig. 6 both $m_{\omega y}$ and κ_y computed from (8.10) display the so-called edge effect with rapid attenuation. At the midspan ($\xi = 1$) from (8.10)

$$\kappa_y(1) = \frac{\alpha}{2}\bar{p}^*_{s4} \qquad m_{\omega y}(1) = -\frac{1}{4\alpha}\bar{p}^*_{s4}.$$

Consequently, from (6.9) also for $\xi = 1$

$$P_4 = m_\omega \frac{EI_\omega}{Ll} = -\frac{P^*_{s4}L}{4\alpha}; \qquad V_4 = \frac{\kappa I_\omega}{JlL^3} = \frac{\alpha P^*_{s4}}{2EJL}.$$

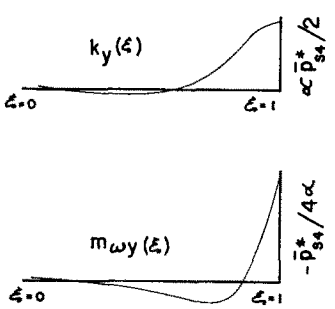

Fig. 6. Diagram of cross-sectional flattening κ_y and the bimoment $m_{\omega y}$ (on the left half of the shell) due to two concentrated loads $Q^*_{1y} = Q^*_{6y} = Q^*$ at $\xi = 1$.

† Implied is, actually, that the external load has, among others, the $p^*_4 = P^*_{s4}\delta(z - L/2)$ component.

Now we can compute stresses associated with the cross-sectional distortion (last term in 6.3). At the midspan ($\xi = 1$) and for $y = \pm h$

$$\sigma_z^{(d)} = \frac{P_4}{I_\omega}\Phi_4\bigg|_{\pm h} = -\frac{P_{s4}^* L}{6\alpha d l^3}. \tag{8.11a}$$

The bending moment $M_s^{(v)}$ in the "frame" $\xi = 1$, associated with the "flattening" $V_4\Psi_4$ is from (4.2)

$$M_s^{(v)} = \frac{24}{5}\frac{EIh}{l^2}V_4 = \frac{\alpha h}{24Ll}P_{s4}^*.$$

Consequently, using (6.12) the normal hoop stresses in all of the nodes

$$\sigma_s^{(v)} = \frac{N_s}{d} + \frac{M_s d}{2I} = \frac{p_{si}}{d} \pm \frac{3\alpha l}{16hd^2L}P_{s4}^*. \tag{8.11b}$$

We notice that for long and thin shells

$$\alpha \approx \beta \approx \frac{s}{\sqrt{2}} = \frac{L}{l}\left(\frac{16d^2}{5l^2}\right)^{1/4}. \tag{8.12}$$

Hence, from (8.11) it follows that in case of concentrated distortional loads P_{s4}^*

$$\begin{aligned}\sigma_z^{(d)} &= -\frac{1}{6}(ld)^{-3/2}\left(\frac{5}{16}\right)^{1/4}P_{s4}^* \\ \sigma_s^{(v)} &= \frac{p_{si}}{d} \pm \frac{\sqrt{3}}{8}(ld)^{-3/2}\left(\frac{16}{5}\right)^{1/4}P_{s4}^*.\end{aligned} \tag{8.13}$$

A significant consequence of the stress formulas (8.13) is that neither $\sigma_z^{(d)}$ nor $\sigma_s^{(v)}$ depend on the span L and on boundary conditions at the edges. Hence, as a result of the edge effect behavior of the cross-sectional distortion the normal stresses computed from (8.13) are simply added to the stresses computed from the conventional beam theory (as derived in 6.3) regardless of boundary conditions.

8.1 *Loading case A*

Consider first the case of two vertical point loads $Q_{1y}^* = Q_{6y}^* = Q^*$. From Table 1 (top line) $p_{s1} = 2Q^*$ and $p_{s4} = 2hQ^*$ are the only two non-vanishing load terms. The normal beam stress at midspan and for $y = \pm h$ for a simply supported shell at both edges is

$$\sigma_z^{(b)} = \mp\frac{M_z}{I_x}h = \mp\frac{\sqrt{3}}{10}\frac{L}{dl^2}Q^*;\ \sigma_s^{(b)} = 0.$$

Thus, using (8.13a) the longitudinal normal stress σ_z at $y = \pm h$, $z = L/2$ is simply

$$\sigma_z = \sigma_z^{(b)} + \sigma_z^{(d)} = \left[\mp\frac{\sqrt{3}}{10}\frac{L}{dl^2} - 0.217l(dl)^{-3/2}\right]Q^* \tag{8.14}$$

while at $y = 0$, since $\sigma_z^{(b)} = 0$

$$\sigma_z = 0.434l(\mathrm{d}l)^{-3/2}Q^*.$$

Since the load is applied at nodes the local bending moments of the pinned frame $M_s^{(l)}$ are zero everywhere. Consequently, the only remaining component of the normal hoop stress is computed from (8.13b). Maximum normal force is in the upper flat $p_{s(16)} = -2\frac{\sqrt{3}}{3}Q^*$ such that

$$\sigma_s = \left[-1.155\frac{1}{bd} \mp 0.502l(\mathrm{d}l)^{-3/2}\right]Q^* \tag{8.15}$$

where $b = 1.0$ is the unit width of the frame. Upper sign refers to the outside surface.

In order to verify the analytical results a 316 SS stainless steel control rod thimble was straingauged while the loading was controlled from an Instron testing machine. Altogether 33 90° tee rosettes and delta type straingauges were used and the loading was slowly incremented by 20 lb. The geometrical parameters of the shell were $L = 60$ in., $l = 1.301$ in. and $d = 0.04$ in.†

The same shell was analyzed using the Solid Sap[14] finite element program. Due to the symmetry only one quarter (divided into 480 elements) of the shell was analyzed.†

It turns out that the normal stresses σ_z as computed from (8.14) are in very close agreement with both test and computer results. At $z = L/2$ the extremum stresses σ_z (in the top and bottom flat) are for $Q^* = 100$ lb

Test	$\sigma_{z\,\min,\,\max} = (-18150;\ 12900)$ psi,
Finite elements	$\sigma_{z\,\min,\,\max} = (-17930;\ 14300)$ psi,
Formula (8.14)	$\sigma_{z\,\min,\,\max} = (-18000;\ 13250)$ psi.

As expected the correlation is not as good for circumferential stresses. However, the results are still quite good‡ for all technical purposes as shown in Table 2.

Table 2. Circumferential normal stresses σ_s (in psi) for $Q_{1y}^* = Q_{6y}^* = 100$ lb at $z = L/2$

σ_s(psi)	$(x, y) = (0, -h)$ In‖	Out‖	$(x, y) = (l/2, -h)$ In	Out	$(x, y) = (-l, 0)$ In	Out
Test†		−9750				6600
Finite elements	§2265	−7235	2465	−7035	−8160	8080
Equation (8.14)	2620	−8390	2620	−8390	−5500	5500

† Not all available.
§ Extrapolated from results computed in the middle of each element.
‖ Surface of the plate.

We note also that the decaying nature of cross-sectional distortion, i.e. stresses $\sigma_z^{(d)}$ and $\sigma_s^{(v)}$, was confirmed by both test and computer results.

† For more details see Appendices A and B.
‡ For an elasticity type of solution of a two plate folded structure one may consult two papers by Dundurs and Samuchin [15, 16].

8.2 *Loading case B*

In order to test the method on a case exhibiting local bending of the "frame," examined is the same shell loaded by a vertical point force $Q^* = 20$ lb applied in the middle of the top flat† $(x, y, z = 0, -h, L/2)$.

Diagram of local bending moments $M_s^{(l)}$ is shown in Fig. 7 and the generalized loads computed from reactions are $\bar{p}_1 = Q^*$ (vertical transverse force) and $P_4^* = \frac{3}{2}hQ^*$.

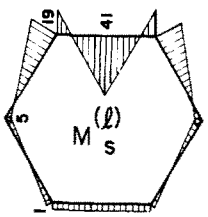

Fig. 7. Bending moments in frame pinned at all six nodes due to the unit normal force in the middle of the upper flat. Moments multiplied by $240/Q^*l$.

The longitudinal normal stress in the top (away from the force) and bottom flat computed using finite elements $\sigma_{z,\,\min\,\max} = (-1740, 1255)$ psi and formula (8.14) $\sigma_{z,\,\min\,\max} = (-1740, 1380)$ psi are again in good agreement. In order to compute the normal stess σ_z directly under the concentrated force the local bending of the upper plate has to be accounted for. From [17] (Chap. 35) the bending moment $M_x^{(l)}$ directly under a central force Q^* distributed over a small circle with radius c is

$$M_x^{(l)} = \frac{Q^*}{4\pi}\left[(1+\nu)\log\frac{2l}{\pi c} - \nu\right]. \tag{8.16}$$

With $c = 0.1\ l$ (corresponding roughly to the actual loading device) from (8.16) $M_x^{(l)} = 3.35$ lb and $\sigma_z^{(l)} = \pm 12570$ psi. Hence, $\sigma_{z,\,\min} = -12570 - 1740 = -14310$ psi which agrees well with the value $\sigma_{z,\,\min} = -13860$ psi recorded in tests. Finite element results are not quite reliable due to the extrapolation involved.

The circumferential normal stresses σ_s at $z = L/2$ are associated with distortion (flattening) (8.13b) and local bending Fig. 7 (since the external load is not applied at node). At $(x, y) = (0, -h)$ the local bending moment $M_s^{(l)} = 41\ Q^*l/240 = 22.2$ lb. Thus, $\sigma_s = \mp 16650 \mp 830 = \mp 17480$ psi, where the second term $\sigma_s^{(v)}$ is the contribution of the flattening (i.e. nodal force P_4^*). Results for normal hoop stresses σ_s at $z = L/3$ are arranged in Table 3.

Table 3. Circumferential normal stresses σ_s (psi) for a concentrated point load $Q_y^* = 20$ lb at $(x, y, z = 0, -h, L/2)$

σ_s(psi)	$(x, y) = (0, -h)$ In	Out	$(x, y) = (-l, 0)$ In	Out	$(x, y) = (0, h)$ In	Out
Test	16200			480		−570
Finite elements	(not extrapolated)		−425	440	460	−460
Present model	17480	−17480	−200	200	520	−520

† One is reminded that the shell theory in general is not suited for the analysis of point loads. This model may in fact have a better chance using frames and lattices as elements.

The accuracy of the results from the present model are good enough for all practical purposes. The rather larger percentage error at $(x, y) = (-l, 0)$ is not very significant because the stress level is low (i.e. the absolute error of only 280 psi is not disturbing).

8.3 *Distributed loading*

Another very common type of loading is uniformly distributed load over entire (or part of the) surface of the upper flat. Let us consider the case of load p_n (perpendicular to the middle surface) uniformly distributed over the entire upper flat ($0 \le z \le L$; $-l/2 \le x \le l/2$; $y = -h$). As shown in the beginning of this Section, load p_n is first resolved into components p^*_{s1} and p^*_{s4} (8.1). Next, the particular integral vector is computed from (7.5) for this specific loading as

$$\{s^0\} = p^*_{s4} \begin{Bmatrix} \Delta(\alpha F_1 - \beta F_3) \\ F_2 + \gamma F_4 - 1 \\ -F_4/2\alpha\beta \\ (\alpha F_1 + \beta F_3)/2\alpha\beta \end{Bmatrix}. \tag{8.17}$$

All functions F_i are computed for $\xi = 1$. For a shell free to distort at both ends (8.2) $m_{\omega y} = q_y = 0$ at both ends $\xi = 0, 1$. Hence, from (7.1 3) it follows

$$\begin{bmatrix} (\alpha^2 + \beta^2)(\beta F_1 - \alpha F_3) & -F_4 \\ (\alpha^2 + \beta^2)^2 F_4 & \alpha F_1 + \beta F_3 \end{bmatrix} \begin{Bmatrix} \omega^0_y \\ \kappa^0_y \end{Bmatrix} = p^*_{s4} \begin{Bmatrix} -F_4 \\ \alpha F_1 + \beta F_3 \end{Bmatrix}. \tag{8.18}$$

By inspection from (8.18)

$$\omega^0_y = 0 \qquad \kappa^0_y = p^*_{s4}$$

Thus, $\omega_y \equiv m_{\omega y} \equiv q_y \equiv 0$ over the entire span while $\kappa_y = p^*_{s4} = \text{const}$. Note that the same result can be deduced directly from (6.10).

The conclusion is that a cross-section of an unstiffened shell subjected to uniformly distributed load p_n (psi) over the entire surface of the upper flat distorts only in its own plane, i.e. flattens uniformly ($\kappa_y = \text{const.}$) without warping ($\omega_y \equiv 0$). The same conclusion is valid for the central part of a long stretch of shell loaded uniformly (as a consequence of a rapid decay of discontinuities—edge effect).

Normal stress σ_z has only the conventional beam bending component $\sigma_z = M_z y/2I_y$, while the hoop normal stress σ_s is a function of the circumferential coordinate only, $\sigma_s = \sigma_s(s)$. Bending moment diagram $M^{(l)}_s$ associated with the local bending of the supported hex "frame" is shown in Fig. 5(a). Due to the distortional load p^*_{s4} (8.1b)

$$V_4 = \kappa \frac{I_\omega}{JlL^3} = \frac{p^*_{s4}}{EJ}$$

and

$$M^{(v)}_s = \frac{24}{5} \frac{EIh}{l^2} V_4 = \frac{24}{5} \frac{Ih}{Jl^2} p^*_{s4}$$

in each node. Thus, the maximum hoop normal stress due to the flattening is

$$\sigma^{(v)}_s = \mp \frac{M^{(v)}_s}{2I} d = \mp \frac{1}{2} \left(\frac{l}{d}\right)^2 p_n \tag{8.19}$$

at the top and bottom flat (upper sign for outer surface) and at $(x, y) = (\pm l, 0)$. The extreme circumferential normal stress is

$$\sigma_s = \mp \frac{19}{45} \frac{p_n l^2}{8} \frac{d}{2I} \mp \frac{1}{2} \left(\frac{l}{d}\right)^2 p_n = \mp \left(\frac{19}{60} + \frac{1}{2}\right) \left(\frac{l}{d}\right)^2 p_n$$

or finally

$$\sigma_{s,\,\max\,\min} = \pm 0.817 \left(\frac{l}{d}\right)^2 p_n. \tag{8.20}$$

Consequently, knowing the beam solution for σ_z and computing the hoop normal stress σ_s from (8.20) suffices for the proportioning of a shell subjected to a uniformly distributed pressure p_n along the entire (or a large part of) surface of the upper flat.

The application of the method to other cases of loading and support condition is straightforward since the general algorithm is always substantially similar to one demonstrated in this Section.

9. SUMMARY

In conclusion, the proposed elastic analysis of polygonal shells with hexagonal cross section subjected to an arbitrary system of lateral and longitudinal loads appears to be both straightforward and accurate enough for all practical purposes. For most cases of interest for a practical designer the stresses are given in terms of simple formulas allowing not only for rapid computation but also for an easy structural optimization procedure.

In view of the results presented it appears that the method has the accuracy comparable to the finite element method with a sizable number of elements. Hence, only for very serious problems demanding high level of accuracy it appears justified to employ the finite element method with an extraordinary fine mesh. The demand for such as accuracy may, however, be questioned in light of uncertainties concerning the material properties, load and manufacturing imperfections.

Finally, although the presented procedure is derived exclusively for polygonal shells with hexagonal cross-section it would be rather straight-forward to extend it to shells with cross-sections in the form of other polygons.

REFERENCES

1. E. H. Baker, L. Kovalevsky and F. L. Rish, *Structural Analysis of Shells*. McGraw-Hill, New York (1972).
2. Phase I Report on Folded Plate Construction, Report of the Task Committee on Folded Plate Construction. *J. Struct. Div. ASCE* **89**, 365 (1963).
3. W. Fluegge, *Stresses in Shells*. Springer, Berlin (1960).
4. C. Meyer and A. C. Scordelis, Computer program for prismatic folded plates with plate and beam elements. U. of California Berkeley, *Rep.* UC SESM 71-23 (1970).
5. J. E. Flinn, D. Krajcinovic *et al.*, Evaluation of ex-reactor loading event in the high fluence control-rod thimble 5E3. EBR-II Project, *Final Report*, November (1972).
6. D. Krajcinovic, Stress analysis of hexagonal shells, *Int. J. Solids Struct.* 7, 559 (1971).
7. V. Z. Vlasov, *General theory of shells and its applications in engineering*. Part V, NASA Transl. N64-19883, Washington (1964).
8. V. V. Novozhilov, *The Theory of Thin Shells*, Chap. 3. Noordhoff, Groningen (1959).
9. I. F. Obrazcov, *Variational methods of analysis of thinwalled airplane structures* (in Russian). Mashinostroenie, Moscow (1966).
10. K. Girkmann, *Flaechentragwerke*. Springer, Berlin (1959).
11. L. V. Kantorovich and V. I. Krylov, *Approximate Methods of Higher Analysis*, Chap. 4.3. Noordhoff, Groningen (1958).

12. C. F. Kollbrunner and N. Hajdin, Die St.-Venantsche Torsion. Mitt. der *Tech. Komm.*, Schweizer Stahlban-Ver., Heff 26, Zurich (1963).
13. E. C. Pestel and F. A. Leckie, *Matrix Methods in Elastomechanics*. McGraw-Hill, New York (1963).
14. E. L. Wilson, Solid Sap. Univ. of California Berkeley, *Rep.* UC SESM 71-19 (1971).
15. J. Dundurs and M. G. Samuchin, Transmission of concentrated forces into prismatic shells—I. *Int. J. Solids Struct.* **7**, 1627 (1971).
16. M. G. Samuchin and J. Dundurs, Transmission of concentrated forces into prismatic shells—II. *Int. J. Solids Struct.* **9**, 269 (1973).
17. S. Timoshenko and S. Woinowsky-Krieger, *Theory of Plates and Shells*. McGraw-Hill, New York (1959).

Абстракт — На основе теории полумембранных оболочек развита новая дискретно-непрерывная аналитическая модель для призматических оболочек с гексагональным сечением. Окончательные результаты для напряжений выведены в виде простых выражений. Предположенная аналитическая модель проверена в отношении к результатам экспериментов и методу конечных элементов. Судя по всем рассмотренным случаям, точность оказывается чрезвычайно хорошим. Поэтому, повидимому, метод обеспечит простое, но сильное орудие при проектировании каналов узлов ядерных реакторов.